

Chimeras and clusters emerging from robust-chaos dynamics

M. G. Cosenza,^{1,2} O. Alvarez-Llamoza,³ and A. V. Cano^{4,5}

¹*School of Physical Sciences & Nanotechnology, Universidad Yachay Tech, Urcuquí, Ecuador*

²*Universidad de Los Andes, Mérida, Venezuela*

³*Grupo de Simulación, Modelado, Análisis y Accesabilidad,
Universidad Católica de Cuenca, Cuenca, Ecuador*

⁴*Institute for Integrative Biology, ETH, Zurich, Switzerland*

⁵*Swiss Institute of Bioinformatics, Lausanne, Switzerland*

(Dated: February 2021)

ABSTRACT

We show that dynamical clustering, where a system segregates into distinguishable subsets of synchronized elements, and chimera states, where differentiated subsets of synchronized and desynchronized elements coexist, can emerge in networks of globally coupled robust-chaos oscillators. We describe the collective behavior of a model of globally coupled robust-chaos maps in terms of statistical quantities, and characterize clusters, chimera states, synchronization, and incoherence on the space of parameters of the system. We employ the analogy between the local dynamics of a system of globally coupled maps with the response dynamics of a single driven map. We interpret the occurrence of clusters and chimeras in a globally coupled system of robust-chaos maps in terms of windows of periodicity and multistability induced by a drive on the local robust-chaos map. Our results show that robust-chaos dynamics does not limit the formation of cluster and chimera states in networks of coupled systems, as it had been previously conjectured.

I. INTRODUCTION

Many smooth nonlinear dynamical systems possess chaotic attractors embedded with a dense set of periodic orbits for any range of parameter values. Therefore, in practical systems operating in chaotic mode, a slight perturbation of a parameter may drive the system out of chaos. Alternatively, there exist dynamical systems that exhibit the property of robust chaos [1–6]. A chaotic attractor is said to be robust if, for its parameter values, there exists a neighborhood in the parameter space where windows of periodic orbits are absent and the chaotic attractor is unique [1].

Robust chaos constitutes an advantageous feature in applications that require reliable functioning in a chaotic regime, in the sense that the chaotic behavior cannot be removed by arbitrarily small fluctuations of the system parameters. For instance, networks of coupled maps with robust chaos have been efficiently used in communication and encryption algorithms [7] and they have been investigated for information transfer across scales in complex systems [8]. In addition, the existence of robust chaos allows for heterogeneity in the local parameters of a system of coupled oscillators, while guaranteeing the performing of all the oscillators in a chaotic mode.

On the other hand, systems possessing robust chaos may present limitations in the types of collective behaviors that they can achieve, in comparison with systems displaying periodic windows. For example, it has been conjectured that the phenomenon of dynamical clustering in globally coupled networks (where the system segregates into distinguishable subsets of synchronized elements) is only found when stable periodic windows are present in the local elements [9–11]. Recently, it has also

been argued that chimera states (i.e., coexistence of subsets of oscillators with synchronous and asynchronous dynamics) cannot emerge in networks of coupled oscillators having robust chaotic attractors [12, 13].

The phenomenon of dynamical clustering is relevant as it can provide a simple mechanism for the emergence of differentiation, segregation, and ordering of elements in many physical and biological systems [14, 15]. Clustering has been found in systems of globally coupled Rössler oscillators [16], neural networks [17], biochemical reactions [18], and has been observed experimentally in arrays of globally coupled electrochemical oscillators [19] and globally coupled salt-water oscillators [20]. In addition, the study of chimera states currently attracts much interest; for reviews see, [21, 22]. Chimera states have been found in networks of nonlocally coupled phase oscillators [23, 24], in systems with local [25–28] and global [29–34] interactions, and in networks of time-discrete maps [35–38]. These states have been investigated in a diversity of contexts [39–47]. Chimera states have been observed in experimental settings, such as populations of chemical oscillators [48], coupled lasers [49], optical light modulators [50], electronic [51], and mechanical [52, 53] oscillator systems. It has been shown that clustering is closely related to the formation of chimera states in systems of globally coupled periodic oscillators [31].

In this paper, we investigate the occurrence of dynamical clustering and chimera states in systems of coupled robust-chaos oscillators. In Sec. II, we describe the characterization of synchronization, cluster and chimera states in globally coupled systems. In Sec. III we consider a network of globally coupled robust-chaos maps and show that cluster and chimera states can actually emerge in this system for several values of parameters.

In Sec. IV, we employ the analogy between the local dynamics of the globally coupled system with the response dynamics of a single driven map. We interpret the occurrence of clusters and chimeras in the globally coupled system in terms of windows of periodicity induced by the drive on the local robust-chaos map. Conclusions are presented in Sec V.

II. METHODS

A global interaction in a system can be described as a field or influence acting on all the elements in the system. As a simple model of an autonomous dynamical system subject to a global interaction, we consider a system of N maps coupled in the form

$$x_{t+1}^i = (1 - \epsilon)f(x_t^i) + \epsilon h_t(x_t^j | j \in S), \quad (1)$$

where x_t^i ($i = 1, 2, \dots, N$) describes the state variable of the i th map in the system at discrete time t , the function f expresses the local dynamics of the maps, the function h_t represents a global field that depends on the states of the elements in a given subset S of the system, at time t , and the parameter ϵ measures the strength of the coupling of the maps to the field. The form of the coupling in Eq. (1) is assumed in the commonly used diffusive form. The function h_t may not depend on all the elements, but it must be shared by all the elements of the system to be a global interaction.

A collective state of synchronization or coherence takes place in the system Eq. (1) when $x_t^i = x_t^j$, $\forall i, j$ for asymptotic times. A desynchronized or incoherent state corresponds to $x_t^i \neq x_t^j$ $\forall i, j$ for all times. Dynamical clustering occurs when the system segregates into a number of K distinct clusters or subsets of elements such that elements in given subset are synchronized among themselves. In other words, $x_t^i = x_t^j = X_t^\xi$, $\forall i, j$ in the ξ th cluster, where X_t^ξ denotes the value of x_t^i in that cluster, with $\xi = 1, \dots, K$. If n_ξ is the number of elements belonging to the ξ th cluster, then its relative size is $p_\xi = n_\xi/N$. In general, the number of clusters, their size, and their dynamical evolution (periodic, quasiperiodic, or chaotic) depend on the initial conditions and parameters of the system. A chimera state consists of the coexistence of one or more clusters and a subset of desynchronized elements. If there are K clusters, the fraction of elements in the system belonging to clusters is $p = \sum_{\xi=1}^K n_\xi/N$ while $(1 - p)$ is the fraction of elements in the desynchronized subset.

In practical applications, we consider that two elements i and j belong to a cluster at time t if the distance between their state variables, defined as

$$d_{ij}(t) = |x_t^i - x_t^j|, \quad (2)$$

is less than a threshold value δ , i.e., if $d_{ij} < \delta$. The choice of δ should be appropriate for achieving differentiation

between closely evolving clusters. Then, we calculate the fraction of elements that belong to some cluster at time t as [16]

$$p(t) = 1 - \frac{1}{N} \sum_{i=1}^N \prod_{j=1, j \neq i}^N \Theta[d_{ij}(t) - \delta], \quad (3)$$

where $\Theta(x) = 0$ for $x < 0$ and $\Theta(x) = 1$ for $x \geq 0$. We refer to p as the asymptotic time-average of $p(t)$. Then, a clustered state in the system can be characterized by the value $p = 1$, while an incoherent state in the system corresponds to $p \rightarrow 0$. The values $p_{\min} < p < 1$ characterize a chimera state, where p_{\min} is the minimum cluster size to be taken into consideration.

A synchronization state corresponds to the presence of a single cluster of size N and has also the value $p = 1$. To distinguish a synchronization state from a multicluster state, we calculate the asymptotic time-average $\langle \sigma \rangle$ as

$$\langle \sigma \rangle = \frac{1}{T - \tau} \sum_{t=\tau}^T \sigma_t, \quad (4)$$

where τ is the number of discarded transients, T is a sufficiently large time, and σ_t is the instantaneous standard deviation of the distribution of state variables defined by

$$\sigma_t = \left[\frac{1}{N} \sum_{i=1}^N (x_t^i - \bar{x}_t)^2 \right]^{1/2}, \quad (5)$$

where

$$\bar{x}_t = \frac{1}{N} \sum_{j=1}^N x_t^j. \quad (6)$$

Statistically, a synchronization state is characterized by the values $\langle \sigma \rangle = 0$ and $p = 1$, while a cluster state corresponds to $\langle \sigma \rangle > 0$ and $p = 1$. Chimera states are characterized by $\langle \sigma \rangle > 0$ and $p_{\min} < p < 1$, and desynchronization is described by $\langle \sigma \rangle > 0$, $p < p_{\min}$. In this paper we set $\delta = 10^{-6}$ and $p_{\min} = 0.05$.

Note that, in systems with local or long-range interactions where there is a natural spatial ordering, the synchronized and desynchronized domains for chimera states are localized in space. In contrast, globally coupled systems lack the notion of spatial order. Thus, the of chimera and cluster states in our system are characterized in terms of the statistical quantities $\langle \sigma \rangle$ and p , not on the spatial location of synchronized and desynchronized domains.

III. RESULTS AND DISCUSSION

Chimeras and clusters in globally coupled robust chaos maps

Let us consider a network of globally coupled maps described by the equations [14]

$$x_{t+1}^i = (1 - \epsilon)f(x_t^i) + \frac{\epsilon}{N} \sum_{j=1}^N f(x_t^j), \quad (7)$$

where the global interaction function is the mean field of the system,

$$h_t = \frac{1}{N} \sum_{j=1}^N f(x_t^j). \quad (8)$$

As local dynamics exhibiting robust chaos, we consider the following smooth, unimodal map defined on the interval $x \in [0, 1]$ [54],

$$x_{t+1} = f(x_t) = \frac{1 - b^{(1-x_t)x_t}}{1 - b^{1/4}}. \quad (9)$$

which is chaotic with no periodic windows on the parameter interval $b \in [0, 1]$. On this interval, the Lyapunov exponent of map Eq. (9) has the constant value $\lambda = \ln 2$. The bifurcation diagram of map Eq. (9) in Figure 1 shows the absence of periodicity in the interval $b \in [0, 1]$.

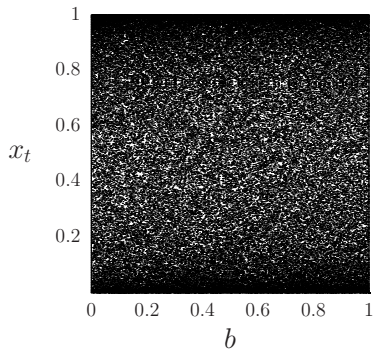


FIG. 1. Bifurcation diagram of the map Eq. (9) as a function of the parameter b .

Figure 2 shows the asymptotic temporal evolution of the states of the system Eqs. (7) and (9), for different values of parameters. Since the system is globally coupled, there is no natural spatial ordering. For visualization purposes, the indexes i are ordered at time $t = 10^4$ such that $i < j$ if $x_t^i < x_t^j$ and kept fixed afterwards. The values of the states x_t^i are represented by distinct color coding; two elements i, j share the same color if $x_t^i = x_t^j$. A desynchronized state is displayed in Fig. 2(a) and a complete synchronization state occurs in Fig. 2(d), while a chimera state and a two-cluster state are visualized in Figs. 2(b) and 2(c), respectively.

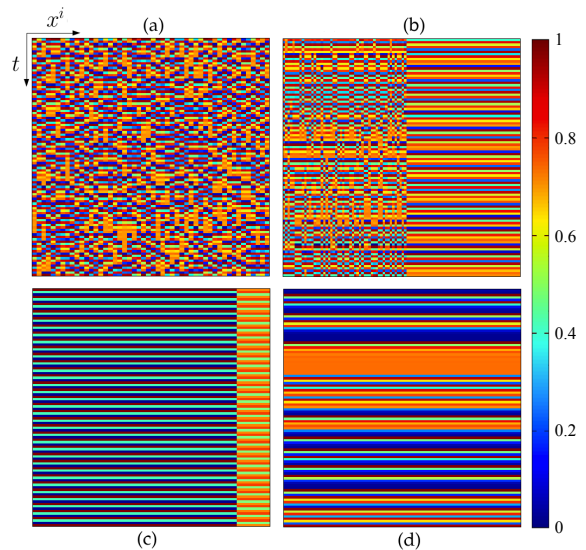


FIG. 2. Asymptotic evolution of the states x^i (horizontal axis) as a function of time (vertical axis) for the system Eqs. (7) and (9) with size $N = 100$ and fixed $b = 0.5$, for different values of the coupling parameter. Random initial conditions are uniformly distributed in the interval $[0, 1]$. After discarding 10^4 transients, 100 iterates t are displayed. Ordering of the map indexes is explaining in the text. Color code: two elements i, j share the same color if $x_t^i = x_t^j$. (a) Incoherent or desynchronized state, $\epsilon = 0.15$. (b) Chimera state, $\epsilon = 0.2$. (c) Two-cluster state, $\epsilon = 0.39$. (d) Synchronization, $\epsilon = 0.6$.

Figure 3 shows the collective states arising in the system Eqs. (7) and (9) on the space of parameters (ϵ, b) , characterized through the quantities p and $\langle \sigma \rangle$. Labels indicate the regions where these behaviors occur: CS: complete synchronization; C: cluster states; Q: chimera states, and D: desynchronization.

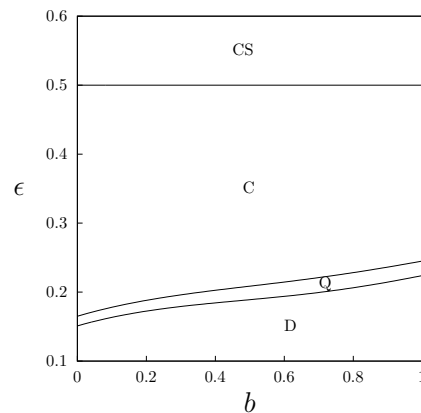


FIG. 3. Phase diagram on the plane (ϵ, b) for the autonomous system Eqs. (7) and (9) with size $N = 500$. For each data point, the quantities p and $\langle \sigma \rangle$ are obtained by averaging over 50 realizations of random initial conditions x_0^i uniformly distributed in the interval $[0, 1]$. Labels indicate different collective states. CS: synchronization; C: cluster states; Q: chimera states; D: desynchronization.

The linear stability analysis for the complete synchronization state in the globally coupled system Eq. (7) shows that this state is stable if the following condition is satisfied [14],

$$|(1 - \epsilon)e^\lambda| < 1, \quad (10)$$

where λ is the Lyapunov exponent for the local map $f(x)$. For the map Eq. (9), we obtain that the completely synchronized state is stable for $1/2 < \epsilon < 3/2$, which agrees with the numerical characterization for this state performed in Fig. 3. Figure 3 reveals that both cluster and chimera states can arise in globally coupled map networks for appropriate values of parameters, even when the individual maps lack periodic windows. Clusters and chimera states regions occur adjacent to each other for an intermediate range of values of the coupling parameter ϵ on the phase diagram of Fig. 3. In fact, chimeras and clusters are closely related collective states in systems subject to global interactions [30]. Chimera states appear to mediate between dynamical clustering and incoherence.

Multicluster chimera states are also possible in systems of globally coupled robust chaos maps. As an illustration, consider the smooth unimodal map [55],

$$f(x_t) = \sin^2(r \arcsin(\sqrt{x_t})), \quad (11)$$

defined on the interval $x_t \in [0, 1]$ for parameter values $r > 1$. Figure (4) shows the bifurcation diagram of the iterates of map Eq. (11) as a function of the parameter r . The dynamics of the map displays robust chaos with no periodic windows for $r > 1$. The Lyapunov exponent is $\lambda = \ln r$ [55].

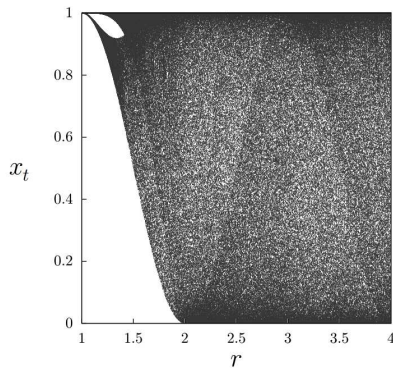


FIG. 4. Bifurcation diagram of the map Eq. (11) as a function of the parameter r .

Figure (5) shows the temporal evolution of the states of the globally coupled system Eqs. (7) with the local map Eq. (11), for different values of parameters. A chimera state with multiple clusters occurs in Fig. 5(a), while a two-cluster state is shown in Fig. 5(b). Multichimera states or multiheaded chimeras (coexistence of multiple localized domains of incoherence and coherence) have been reported in systems with long-range interactions [56]. However, those states are not equivalent to

a chimera state with multiple clusters in a globally coupled system, such as Fig. 5(a), where there is no notion of locality.

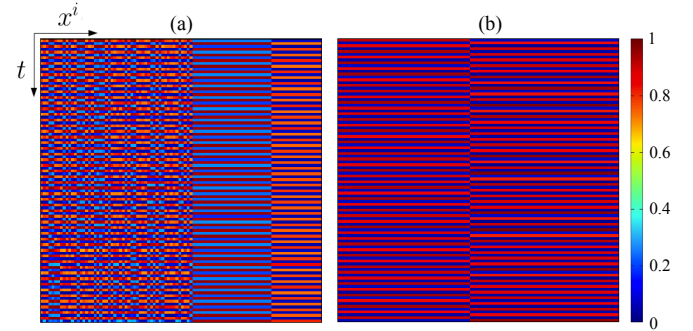


FIG. 5. Asymptotic states x^i (horizontal axis) as a function of time (vertical axis) for the system Eqs. (7) with size $N = 100$ and local map Eq. (11), for different values of parameters. Initial conditions and ordering of the maps are similar to those in Fig. 2. Color code: two elements i, j share the same color if $x_t^i = x_t^j$. (a) Chimera state with two clusters, $r = 3$, $\epsilon = 0.235$. (b) Two-cluster state, $r = 3$, $\epsilon = 0.272$.

Dynamics of clusters and chimera states with global interactions

Consider a chimera state consisting of K clusters and a desynchronized subset in the system of globally coupled maps Eq. (1). The dynamics of this state can be described by the equations

$$\begin{aligned} X_{t+1}^\xi &= (1 - \epsilon)f(X_t^\xi) + \epsilon h_t, & \xi &= 1, \dots, K, \\ x_{t+1}^j &= (1 - \epsilon)f(x_t^j) + \epsilon h_t, & j &= 1, \dots, (1 - p)N. \end{aligned} \quad (12)$$

The mean field Eq. (8) in a chimera state can be expressed as the sum of two contributions

$$h_t = h_C + h_I, \quad (13)$$

where

$$h_C = \sum_{\xi=1}^K p_\xi f(X_t^\xi), \quad (14)$$

$$h_I = \frac{1}{N} \sum_{j=1}^{(1-p)N} f(x_t^j). \quad (15)$$

The term h_C is the contribution to the mean field corresponding to elements belonging to clusters, whereas h_I is the average of the states of the elements belonging to the incoherent subset.

Figure 6 shows the temporal behavior of both contributions h_C and h_I in a chimera state for the globally coupled autonomous system Eqs. (7) and (9). The time evolution of the cluster contribution h_C is chaotic, similar to that of the local map Eq. (9), but h_C has a smaller

amplitude. In general, the form of h_C can be approximated as $h_C \approx Af(y_t)$, where $A < 1$ represents a modulation factor reflecting the partition into several clusters. On the other hand, Fig. 6 reveals that the time series of h_I fluctuates about a mean value with a small dispersion, corresponding to the superposition of the dynamics of many incoherent chaotic elements. Thus, for the given parameter values, the incoherent contribution to the mean field for a large system size can be expressed approximately as a constant; i. e., $h_I \approx k$.

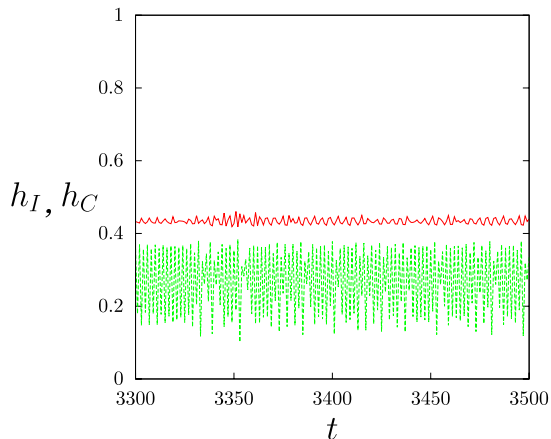


FIG. 6. Cluster h_C (green line) and incoherent h_I (red line) contributions to the mean field of the system Eqs. (7) and (9), as functions of time. Fixed parameters $b = 0.5$, $\epsilon = 0.19$, and size $N = 10^4$.

The dynamics of the globally coupled system Eqs. (1), where each map is subject to a feedback field h_t , can be compared to that of a replica system of maps subject to a global external drive $g(y_t)$ in the form

$$\begin{aligned} x_{t+1}^i &= (1 - \epsilon)f(x_t^i) + \epsilon g(y_t), \\ y_{t+1} &= g(y_t). \end{aligned} \quad (16)$$

It has been shown that an analogy between the autonomous system Eq. (1) and the driven system Eq. (16) can be established when the time evolution of the field h_t is identical to that of the function $g(y_t)$ [9]. Then, the drive-response dynamics at the local level in both systems are similar, and therefore their corresponding emerging collective states can be equivalent for some appropriate parameter values and initial conditions. In particular, chimera or cluster states in the system Eq. (16) should be induced by an external drive function of the form $g(y_t) = Af(y_t) + k$, with A, k constants, that imitates the mean field h_t . The realization of these states depends on the parameters A and k of the drive, and on the coupling strength ϵ .

Figure 7 shows the temporal evolution of the states of the driven system Eqs. (16) with local map Eq. (9), for some values of parameters. A chimera state with a single cluster takes place in Fig. 7(a) for parameter values (ϵ, b) , where chimera states also occur in the autonomous system Eqs. (7) and (9), as seen in the corresponding

phase diagram of Fig. 3. Figure 7(b) shows a two-cluster state for values (ϵ, b) located in the region corresponding to clustered states in Fig. 3. The dynamics of the driven system Eqs. (16) displays multistability; depending on initial conditions, chimeras with different partitions may be induced for given parameters values (ϵ, b) in the region labeled Q in Fig. 3. Similarly, different initial conditions may produce cluster states with different partition sizes for fixed parameter values in region C of Fig. 3.

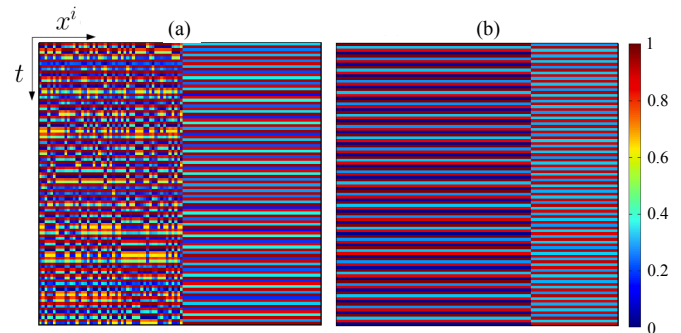


FIG. 7. Asymptotic evolution of the states x^i (horizontal axis) as a function of time (vertical axis) for the driven system Eq. (16) with size $N = 100$ and local map Eq. (9), for different values of the coupling parameter. Fixed values: $A = 0.48$, $k = 0.4$, $b = 0.5$. Random initial conditions x_0^i are uniformly distributed in the interval $[0, 1]$. After discarding 10^4 transients, 100 iterates t are displayed. Ordering of the maps is similar to that in Fig. 2. Color code: two elements i, j share the same color if $x_t^i = x_t^j$. (a) Chimera state; $\epsilon = 0.198$. (b) Two-cluster state; $\epsilon = 0.272$.

The system Eqs. (16) can be considered as N realizations for different initial conditions of a single driven map

$$\begin{aligned} x_{t+1} &= (1 - \epsilon)f(x_t) + \epsilon g(y_t), \\ y_{t+1} &= g(y_t). \end{aligned} \quad (17)$$

Analogously, each local map in the globally coupled system Eqs. (7) can be seen as subject to a field h_t that eventually induces a collective state. Clustering in globally coupled systems of identical elements has been attributed to the existence of periodic windows in the local dynamics [10]. On the other hand, clustering is considered a prerequisite for the occurrence of chimera states in globally coupled systems [31]. Thus, to elucidate the origin of clusters and chimeras in system Eqs. (7) with local robust chaos, one can explore the response dynamics of the single driven map Eq. (17) with a function of the form $g(y_t) = Af(y_t) + k$ and f having robust chaos. Then, if periodic windows are induced by the drive on a single map, one may expect that clusters and chimeras should arise in a globally coupled system of those maps.

Even a trivial function g can modify the dynamics of a driven robust chaos map in Eq. (17) to produce periodic windows. Figure 8(a) shows the bifurcation diagram of x_t in Eq. (17) versus ϵ for the map f given by Eq. (9) with $g(y_t) \rightarrow 0$, which is equivalent to a rescaling of f . Periodic windows typical of unimodal maps appear in

the rescaled map $x_{t+1} = (1 - \epsilon)f(x_t)$. In general, the driven map Eq. (17) represents a rescaling of the robust-chaos map f that acquires periodic windows. Similarly, the periodic cluster states arising in the globally coupled system Eqs. (7) and (9) are a consequence of the windows of periodicity induced locally by the mean field h_t , in analogy to the periodic windows created by an external drive g acting on a single map Eq. (9). Different initial conditions may lead to different out-of-phase orbits with diverse partitions that appear as clusters in the globally coupled system. A synchronization state in the system Eqs. (7) and (9) can be associated to the fixed point interval of the bifurcation diagram of Fig. 8(a), while a desynchronization state in the globally coupled system is a manifestation of a chaotic regime as seen in Fig. 8(a). Nontrivial forms of the driving function can give rise to multistable behavior besides periodic windows. For example, we have verified that a drive such as $g(y_t) = 0.48f(y_t) + 0.4$ in Eq. (17) induces a region of bistability between chaotic attractors that expresses as chimera states in the associated globally coupled system Eqs. (7) and (9).

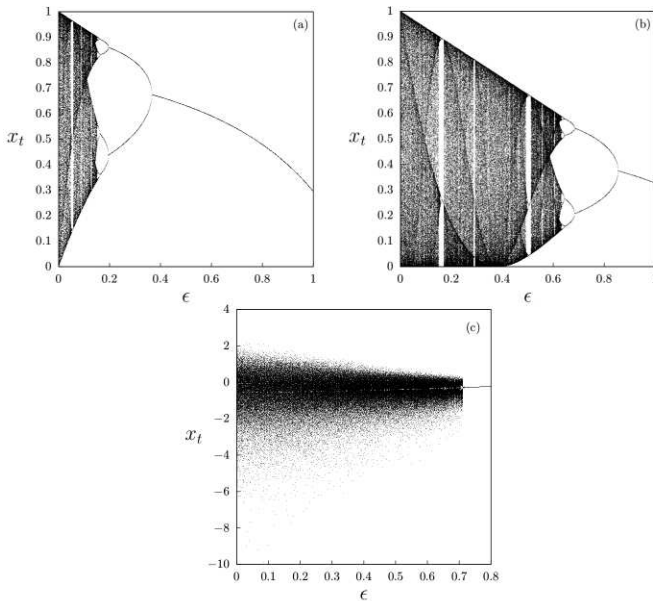


FIG. 8. Bifurcation diagrams of the driven map $x_{t+1} = (1 - \epsilon)f(x_t)$ in Eq. (17) as a function of ϵ for different robust chaos maps f . (a) $f(x) = \frac{1-b(1-x)x}{1-b^{1/4}}$ with $b = 0.5$. (b) $f(x) = \sin^2(r \arcsin(\sqrt{x}))$ with $r = 3$. (c) $f(x) = \ln|x|$.

These results suggest that the emergence of cluster and chimera states in a globally coupled system of robust-chaos maps can be inferred from the occurrence of periodic windows in the response dynamics of a single map subject to an appropriate drive, as a function of parameters. Figure 8(b) shows the corresponding bifurcation diagram of $x_{t+1} = (1 - \epsilon)f(x_t)$ versus ϵ for the map f given by Eq. (11) which also has robust chaos. Again, we see the emergence of periodic windows as the cou-

pling parameter is varied. A globally coupled system of these maps also shows clusters and chimera states, as illustrated in Fig. 5. Figure 8(c) presents the bifurcation diagram of $x_{t+1} = (1 - \epsilon)f(x_t)$ versus ϵ for the logarithmic map $f = a + \ln|x|$, which possesses robust chaos on the parameter interval $a \in [-1, 1]$ and its dynamics is unbounded [2]. In contrast to Figs. 8(a)-(b), no periodic windows appear on the dynamics of the driven map Eq. (17) which remains unbounded; only chaotic orbits and a fixed point attractor appear. As a consequence, clusters and chimera states should not be expected in a globally coupled system of logarithmic maps. In fact, only synchronization and nontrivial collective behavior have been observed in such a system [57].

IV. CONCLUSIONS

Networks of globally coupled identical oscillators are among the simplest symmetric spatiotemporal systems that can display clustering and chimera behavior. Previous works have conjectured that these phenomena cannot occur when the local oscillators possess robust-chaos attractors [9–13]. We have shown that the presence of global interactions can indeed allow for emergence of both cluster and chimera states in systems of coupled robust-chaos maps. Chimeras appear as partially ordered states between synchronization or clustering and incoherent behavior. We have found that chimera states are associated to the formation of clusters in these systems, a feature that has been observed in other globally coupled systems [31].

The existence of intrinsic periodic windows in the dynamics of local oscillators, such as in logistic maps, is not essential for the emergence of clusters with periodic behavior in a globally coupled system of those oscillators. Windows of periodicity and multistability can be induced in the dynamical response of a robust-chaos map subject to an appropriate external forcing. Because of the analogy between a single driven map and the local dynamics of a globally coupled map system, the global interaction field h_t can also induce periodic windows and multistability on local robust-chaos maps. Those are the essential ingredients for the occurrence of cluster and chimera states in globally coupled systems. Since clustering is a prerequisite for chimeras [31], a single driven robust-chaos map that develops periodic windows on some range of parameters allows us to infer that a globally coupled system of such maps shall also exhibit cluster and chimera states on some range of parameters. Conversely, a robust-chaos map, such as the logarithmic or another singular map, that does not give rise to periodic windows when subject to a drive, implies that a system of globally coupled logarithmic or singular maps do not show clusters nor chimera states.

Further extensions of this work include the investigation of chimera states in networks of globally coupled continuous-time dynamical systems possessing ro-

bust chaos or hyperbolic chaotic attractors, the study of interacting populations of robust-chaos elements, and the role of the range of interaction in a network of dynamical robust-chaos units.

ACKNOWLEDGMENT

This work was supported by Corporación Ecuatoriana para el Desarrollo de la Investigación y Academia (CEDIA) through project CEPRA-XIII-2019 “Sistemas Complejos”.

-
- [1] S. Banerjee, J. A. Yorke, and C. Grebogi, *Phys. Rev. Lett.* **80**, 3049 (1998)
 - [2] T. Kawabe and Y. Kondo, *Prog. Theor. Phys.* **85**, 759 (1991).
 - [3] A. Priel and I. Kanter, *Europhys. Lett.* **51**, 230 (2000).
 - [4] A. Potapov and M. K. Ali, *Phys. Lett. A* **277**, 310 (2000).
 - [5] Z. Elhadj and J. C. Sprott, *Front. Phys. China* **3**, 195 (2008).
 - [6] J. A. C. Gallas, *Int. J. Bifurcations & Chaos* **20**, 197 (2010)..
 - [7] P. Garcia, A. Parravano, M. G. Cosenza, J. Jiménez, and A. Marcano, *Phys. Rev. E* **65**, 045201(R) (2002)
 - [8] L. Cisneros, J. Jiménez, M. G. Cosenza, and A. Parravano, *Phys. Rev. E* **65**, 045204(R) (2002).
 - [9] M. G. Cosenza and A. Parravano, *Phys. Rev. E* **64**, 036224 (2001).
 - [10] S. C. Manrubia, A. S. Mikhailov, and D. H. Zanette, *Emergence Of Dynamical Order: Synchronization Phenomena in Complex Systems. World Scientific Lecture Notes in Complex Systems, Vol. 2. World Scientific, Singapore* (2004).
 - [11] R. Charrier, C. Bourjot, and F. Charpillet, In: *European Conference on Complex Systems, Dresden, Germany* (2007).
 - [12] N. Semenova, A. Zakharova, E. Schöll, and V. Anishchenko, *Europhys. Lett.* **112**, 40002 (2015).
 - [13] N. Semenova, A. Zakharova, E. Schöll, and V. Anishchenko, *AIP Conference Proceedings* **1738**, 210014 (2016).
 - [14] K. Kaneko, *Physica D* **41**, 137 (1990).
 - [15] K. Kaneko, *Chaos* **25**, 097608 (2015).
 - [16] D. H. Zanette and A. S. Mikhailov, *Phys. Rev. E* **57**, 276 (1998).
 - [17] D. H. Zanette and A. S. Mikhailov, *Phys. Rev. E* **58**, 872 (1998).
 - [18] Ch. Furusawa and K. Kaneko, *Phys. Rev. Lett.* **84**, 6130 (2000).
 - [19] W. Wang, I. Z. Kiss, and J. L. Hudson, *Chaos* **10**, 248 (2000).
 - [20] K. Miyakawa and K. Yamada, *Physica D* **151**, 217 (2001).
 - [21] E. Schöll, A. Zakharova, and R. G. Andrzejak, *R Chimera States in Complex Networks. Research Topics, Front. Appl. Math. Stat. Lausanne: Frontiers Media SA. Ebook.* (2020).
 - [22] M. J. Panaggio and D. M. Abrams, *Nonlinearity* **28**, R67–R87 (2015).
 - [23] Y. Kuramoto and D. Battogtokh, *Nonlinear Phenom. Complex Syst.* **5**, 380 (2002).
 - [24] D. M. Abrams and S. H. Strogatz, *Phys. Rev. Lett.* **93**, 174102 (2004).
 - [25] C. R. Laing, *Phys. Rev. E* **92**, 050904(R) (2015).
 - [26] M. G. Clerc, S. Coulibaly, M. A. Ferré, M. A. García-Ñustes, and R. G. Rojas, *Phys. Rev. E* **93**, 052204 (2016).
 - [27] B. K. Bera and D. Ghosh, *Phys. Rev. E* **93**, 052223 (2016).
 - [28] J. Hizanidis, N. Lazarides, and G. P. Tsironis, *Phys. Rev. E* **94**, 032219 (2016).
 - [29] G. C. Sethia and A. Sen, *Phys. Rev. Lett.* **112**, 144101 (2014).
 - [30] A. Yeldesbay, A. Pikovsky, and M. Rosenblum, *Phys. Rev. Lett.* **112**, 144103 (2014).
 - [31] L. Schmidt and K. Krischer, *Phys. Rev. Lett.* **114**, 034101 (2015).
 - [32] A. Mishra, S. Saha, C. Hens, P. K. Roy, M. Bose, P. Louodop, H. A. Cerdeira, and S. K. Dana, *Phys. Rev. E* **92**, 062920 (2015).
 - [33] A. V. Cano and M. G. Cosenza, *Phys. Rev. E* **95**, 030202(R) (2017).
 - [34] A. V. Cano and M. G. Cosenza, *Chaos* **28**, 113119 (2018).
 - [35] R. G. Andrzejak, G. Ruzzene, E. Schöll, and I. Omelchenko, *Chaos* **30**, 033125 (2020).
 - [36] I. Omelchenko, B. Riemenschneider, P. Hövel, Y. Maistrenko, and E. Schöll, *Phys. Rev. E* **85**, 026212 (2012).
 - [37] J. Singha and N. Gupte, *Phys. Rev. E* **94**, 052204 (2016).
 - [38] E. V. Rybalova, G. I. Strelkova, and V. S. Anishchenko, *Chaos Solitons & Fractals* **115**, 300 (2018).
 - [39] S. Ulonska, I. Omelchenko, A. Zakharova, and E. Schöll, *Chaos* **26**, 094825 (2016).
 - [40] J. Hizanidis, V. Kanas, A. Bezerianos, and T. Bountis, *Int. J. Bifurcations & Chaos* **24**, 1450030 (2014).
 - [41] V. M. Bastidas, I. Omelchenko, A. Zakharova, E. Schöll, and T. Brandes, *Phys. Rev. E* **92**, 062924 (2015).
 - [42] T. Banerjee, P. S. Dutta, A. Zakharova, and E. Schöll, *Phys. Rev. E* **94**, 032206 (2016).
 - [43] V. Semenov, A. Feoktistov, T. Vadivasova, E. Schöll, and A. Zakharova, *Chaos* **25**, 033111 (2015).
 - [44] N. C. Rattenborg, C. J. Amlaner, and S. L. Lima, *Neurosci. Biobehav. Rev.* **24**, 817 (2000).
 - [45] A. Rothkegel and K. Lehnertz, *New J. Phys.* **16**, 055006 (2014).
 - [46] J. C. González-Avella, M. G. Cosenza, and M. San Miguel, *Physica A* **399**, 24 (2014).
 - [47] A. E. Filatova, A. E. Hramov, A. A. Koronovskii, and S. Boccaletti, *Chaos* **18**, 023133 (2008).
 - [48] M. R. Tinsley, S. Nkomo, and S. Showalter, *Nature Phys.* **8**, 662 (2012).
 - [49] J. D. Hart, K. Bansal, T. E. Murphy, and R. Roy, *Chaos* **26**, 094801 (2016).
 - [50] A. Hagerstrom, T. E. Murphy, R. Roy, P. Hövel, I. Omelchenko, and E. Schöll, *Nature Phys.* **8**, 658 (2012).
 - [51] L. Larger, B. Penkovsky, and Y. Maistrenko, *Phys. Rev. Lett.* **111**, 054103 (2013).

- [52] E. A. Martens, S. Thutupallic, A. Fourrierc, and O. Halatscheka, *Proc. Natl. Acad. Sci. USA* **110**, 10563 (2013).
- [53] K. Blaha, R. J. Burrus, J. L. Orozco-Mora, E. Ruiz-Beltrán, A. B. Siddique, V. D. Hatamipour, and F. Sorrentino, *Chaos* **26**, 116307 (2016).
- [54] M. Andrecut, and M. K. Ali, *Phys. Rev. E* **64**, 025203(R) (2001).
- [55] J. M. Aguirregabiria, *arXiv:0907.3790* (2009).
- [56] I. Omelchenko, O. E. Omelchenko, P. Hövel, Schöll, *Phys. Rev. Lett.* **110**, 224101 (2013).
- [57] M. G. Cosenza and J. González, *Prog. Theor. Phys.* **100**, 21 (1998).